Letter

Probing triaxiality beyond the proton drip line: Spectroscopy of ^{147}Tm

K. Auranen [ORCID],[1,*] P. Siwach,[2] P. Arumugam,[3] A. D. Briscoe,[1] L. S. Ferreira,[4] T. Grahn,[1] P. T. Greenlees,[1] A. Herzáň,[5]
A. Illana,[1,†] D. T. Joss,[6] H. Joukainen,[1] R. Julin,[1] H. Jutila,[1] M. Leino,[1] J. Louko,[1] M. Luoma,[1] E. Maglione,[4]
J. Ojala,[1,‡] R. D. Page,[6] J. Pakarinen,[1] P. Rahkila,[1] J. Romero,[1,6] P. Ruotsalainen,[1] M. Sandzelius,[1]
J. Sarén,[1] A. Tolosa-Delgado,[1] J. Uusitalo,[1,6] and G. Zimba[1]

[1]*Accelerator Laboratory, Department of Physics, University of Jyväskylä, FI-40014 Jyväskylä, Finland*
[2]*Department of Physics, University of Wisconsin-Madison, Madison, Wisconsin 53706, USA*
[3]*Department of Physics, Indian Institute of Technology Roorkee, Roorkee 247667, India*
[4]*Centro de Física e Engenharia de Materiais Avançados CeFEMA, Instituto Superior Técnico, Universidade de Lisboa,
Avenida Rovisco Pais, P1049-001 Lisbon, Portugal*
[5]*Institute of Physics, Slovak Academy of Sciences, SK-84511 Bratislava, Slovakia*
[6]*Department of Physics, Oliver Lodge Laboratory, University of Liverpool, Liverpool L69 7ZE, United Kingdom*

Two triaxial states of the proton-decaying nucleus ^{147}Tm were studied via a comparison of experimental data to results obtained through nonadiabatic quasiparticle calculations. The experimental data were collected in a recoil-decay tagging study using the vacuum-mode recoil separator MARA coupled with the JUROGAM3 γ-ray spectrometer. The previously proposed level scheme above the triaxial $^{11}/2^-$ ($\pi h_{11/2}$) ground state was confirmed, and the level structure was expanded to cover the states above the weakly populated proton-emitting $^5/2^+$ ($\pi d_{5/2}$) isomeric state. It was found that the isomeric state is also triaxial, and possibly more deformed than the ground state.

The amount of energy needed to remove a nucleon from a nucleus is a key quantity that determines the stability of a given isotope. Once this energy becomes negative the neutron or proton drip line has been reached. The nuclei in the proximity of the drip lines provide fundamental information on nuclear matter with extreme proton-neutron ratios. The properties of these nuclei play a key role in the origin of elements [1], as the pathway of the rapid neutron [2] (proton [3–5]) capture process is thought to take place close to the neutron (proton) drip line. Beyond the neutron drip line the least bound neutrons are swiftly emitted, as the nuclear forces are unable to keep them in the proximity of other nucleons. On the opposite extreme of the Segré chart, immediately beyond the proton drip line, protons remain bound to the core by a barrier arising from nuclear, electromagnetic, and centrifugal components, but will eventually escape via tunneling; proton emission has become energetically possible.

Ground-state proton emission [6–11] was found in the early 1980s via the discovery of ^{151}Lu [12], shortly followed by the identification of ^{147}Tm [13] ($T_{1/2} = 0.58(3)$ s [14]). To date, approximately 50 [10] cases of proton emission are known between ^{108}I [5] and ^{185}Bi [15]; the only odd-Z element in between without observed proton emission is promethium. The proton-emission rate is only sensitive to the energy released in the decay Q_p, the angular momentum l_p carried away by the emitted proton, and the shape of the decaying nucleus. Therefore, it is possible to probe the shape of nuclei beyond the proton drip line, even if only a handful of these are produced in an experiment. For example, see Ref. [16] for the recently discovered strongly oblate deformed proton emitter ^{149}Lu. In order to discuss the sign of the quadrupole deformation parameter β_2, or if one follows the Lund convention, the triaxiality parameter γ, the level-spacing in the (rotational) band feeding the proton-emitting state should be measured. This type of measurement has been performed, for example, for the nearby nuclei ^{141}Ho [17], ^{145}Tm [18], and ^{151}Lu [19,20], of which the last one also included lifetime measurements. Alternatively, proton-decay branching ratios ("fine structure") to the excited state of the daughter species may turn out to be very useful. The nonadiabatic quasiparticle model has been used successfully to interpret these data, and to address the shape of proton-emitting nuclei. Whereas ^{151}Lu was concluded to be oblate deformed, ^{140}Ho [21], ^{141}Ho [22], ^{144}Tm [23], and ^{145}Tm [24] were all interpreted to be triaxial in their ground state. Notably, when moving along the proton emitters from the $N = 82$ shell closure toward lighter nuclei, prolate deformation has not been observed, until ^{135}Tb [25].

These results are consistent with other large-scale calculations. For example, the finite-range liquid-drop model [26] and Hartree-Fock-Bogoliubov calculations [27,28] predicted a spherical shape for the even-even nuclei at the closed

---

neutron shell ($N = 82$), but anticipated a moderate oblate deformation ("pumpkin shape") at $N = 80$. Removing further neutrons drives a shape change into complex triaxial forms, and onward towards the neutron midshell, into a strong prolate deformation ("rugby ball shape"). The naïve hypothesis is that a given odd-mass proton emitter adopts the shape of the underlying even-even core. However, atomic nuclei have the intriguing feature that those competing configurations implementing different macroscopic shapes can emerge within a narrow energy range in a given nucleus. This is commonly referred to as shape coexistence [29–33], of which perhaps the most famous example is the triplet of lowest-energy 0^+ states with spherical, oblate, and prolate shapes in ^{186}Pb [34,35].

In this Letter we report the results of an in-beam γ-ray spectroscopy study of ^{147}Tm. The results of a similar study were first reported in Ref. [36], and were later expanded by largely the same authors in Ref. [37]. These studies reported the observation of the favored $\pi h_{11/2}$ ground-state band together with the tentative observation of its unfavored signature partner. A comprehensive theoretical study, using the modified particle-rotor model (MPRM) utilizing the microscopic nonadiabatic quasiparticle approach, was performed in Ref. [38] in order to interpret the ground-state properties of ^{147}Tm. The conclusion was that the MPRM best reproduces the measured data if the nucleus is triaxially deformed with $\beta_2 = 0.21$ and $\gamma = 25°$. In the present work we expanded the level scheme above the weakly populated, proton-decaying low-spin isomeric state, in which only one transition was tentatively placed in Ref. [36]. These results are compared to the MPRM calculations, and we find evidence that the isomeric state is also triaxial, and possibly more deformed than the ground state. This is the first instance when proton decay is used to probe shape coexistence.

The experiment was conducted in the Accelerator Laboratory of University of Jyväskylä, Finland. The nuclei of interest were produced in the ^{92}Mo(^{58}Ni, $p2n$)^{147}Tm fusion-evaporation reaction using a 250-MeV nickel beam with 5 pnA (3×10^{10} ions/s) average beam intensity over an exposure time of 66 h. The 550-μg/cm^2-thick self-supporting target was placed at the center of the JUROGAM3 [39] Compton-suppressed γ-ray spectrometer. The fusion-evaporation residues, colloquially referred to as the recoils hereafter, were selected in MARA (Mass Analyzing Recoil Apparatus [40,41]) from the flux of unwanted ions formed by the unreacted primary beam and other target- and beam-like nuclei. The MARA ion-optical reference was set to a charge state of 25.5 that in practice permitted the collection of recoils with four different charge states simultaneously. At the focal plane of MARA the recoils passed through a multi-wire proportional counter (MWPC) before implantation into a 192×72 strip double-sided silicon strip detector (DSSD) with a thickness and pitch of 159 and 670 μm, respectively. The linear energy response of the DSSD was calibrated using a ^{151}Lu proton-decay activity (offset parameter) and standard α source (gain parameter) containing ^{239}Pu, ^{241}Am, and ^{244}Cm activities. The ^{151}Lu decay data were obtained in an experiment performed prior to the present work [16]. The recoils were distinguished from other implantation events based on the MWPC-DSSD time-of-flight information and on
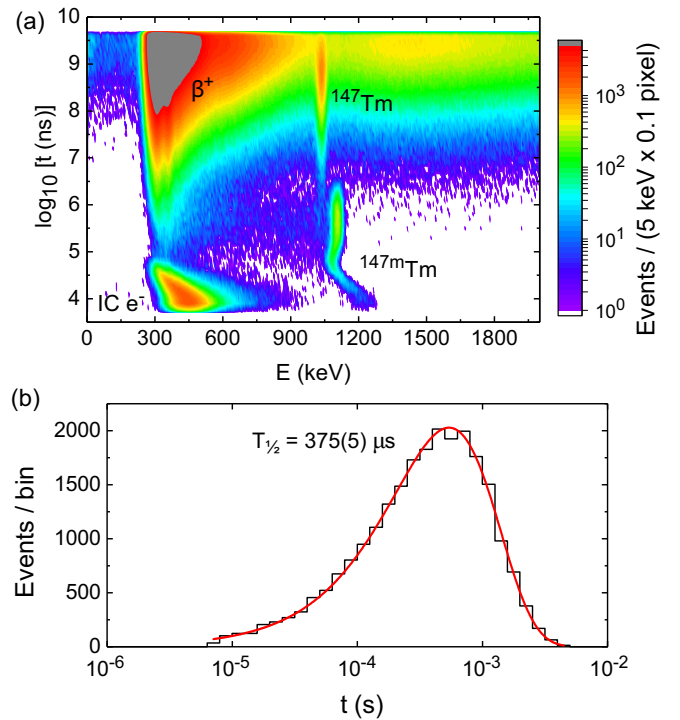

FIG. 1. (a) Energy spectrum of the low-energy decay events versus the recorded decay time. Proton-emission events of ^{147}Tm are labeled together with the internal conversion electrons (IC e^-) and β particles. The fastest ^{147m}Tm events pile up with the preceding recoil event, hence their energy appears higher. The wide ridge at approximately 1500 keV originates from α particles escaping the implantation detector. (b) Decay time distribution of the ^{147m}Tm events. The solid line is a least-squares fit to the data as described in Ref. [43].

the implantation energy. Additionally, an event without the MWPC signal was considered as a decay event. Data from all detector channels were time stamped with a 100-MHz clock, and recorded independently. Finally, data analyses were performed via the GRAIN [42] software package.

The energy spectrum of the recoil correlated low-energy decay events is presented in Fig. 1(a). The two proton-decaying activities of ^{147}Tm are clearly distinguishable, and their intensity ratio suggests that only $\approx 5\%$ of the reactions resulting in ^{147}Tm populate the isomeric state. The extracted proton energies of $E_p(11/2^-) = 1050(5)$ keV and $E_p(5/2^+) = 1120(5)$ keV agree with the evaluated [14] values of 1051(3) and 1119(5) keV, respectively. Due to piling up of the decay signal with that of the preceding recoil implantation event, the measured energies of the fastest ^{147m}Tm events appear higher. The events suffering from the pileup were excluded in the proton-energy analyses. The present data also permit an improved precision on the half-life value of the isomeric $5/2^+$ state of ^{147}Tm, which is important for determining its deformation. A least-squares fit [43] was performed to the decay-time projection of the ^{147m}Tm events, as shown in Fig. 1(b), yielding a half-life of 375(5) μs, which is consistent with the presently recommended value of 360(40) μs [14].

Prompt γ rays feeding the proton-decaying states of ^{147}Tm were probed via the highly selective recoil-decay tagging
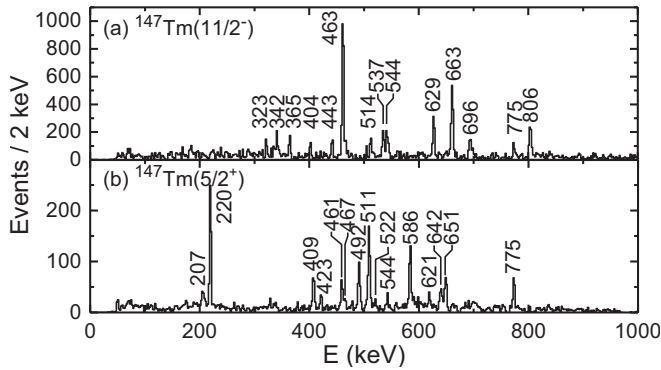
FIG. 2. Singles γ-ray energy spectra tagged with the proton decay of ^{147}Tm (a) $11/2^-$ ground state and (b) $5/2^+$ isomeric state.

technique [44,45]. The acquired singles γ-ray energy spectra are displayed in Fig. 2. As the proton-decay events from the ground state of ^{147}Tm partially overlap with the random background, a background subtraction procedure was introduced. The extracted γ-ray data are listed in the Supplemental Material [46]. Additionally, the coincidence relationships of the γ rays were investigated. Selected examples of the γ-γ coincidence analyses are provided in Fig. 3. The level scheme of ^{147}Tm was constructed based on the above discussed γ-ray data, and it is displayed in Fig. 4.

In this work the proposed [37] level structure above the ground state of ^{147}Tm was confirmed up to the $27/2^-$ state, and the extracted angular distribution coefficients support the suggested spin and parity assignments. Furthermore, the existence of the unfavored signature partner of the ground-state band, tentatively placed in the level scheme in Ref. [37], was confirmed. Based on the systematics along the isotonic chain it was proposed in Ref. [36] that the structure of the
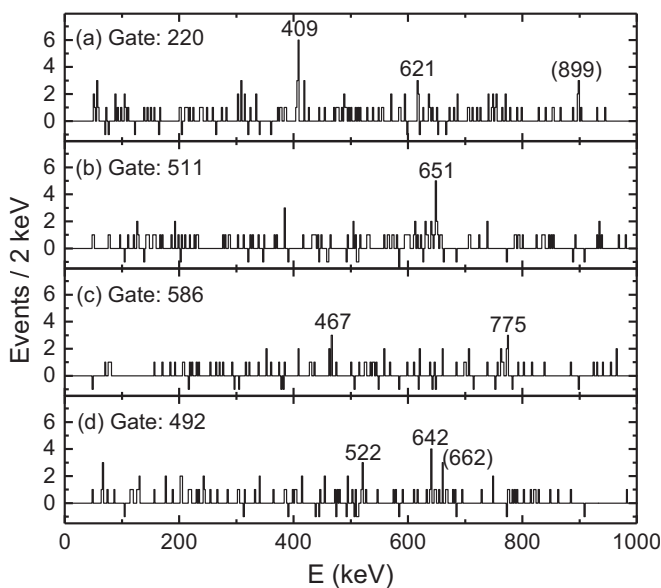

FIG. 3. Examples of γ-γ coincidence analyses when tagging with the proton decay of ^{147m}Tm, and setting a gate on the γ-ray energy as indicated.
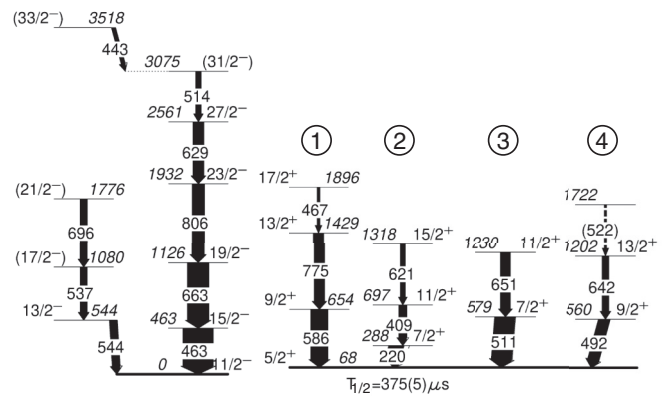

FIG. 4. Level scheme of ^{147}Tm. Intensities of the positive- and negative-parity structures are normalized independently. Excitation energies of the positive parity states inherit a systematic uncertainty of 6 keV [14] arising from the uncertainty of the $5/2^+$ state's energy.

ground-state band is the $h_{11/2}$ proton weakly coupled to the $2^+, 4^+, \ldots$ states of the underlying even-even core. The same reasoning also holds for the states in the unfavored signature partner band. Based on simple particle-rotor calculations, it was found in Ref. [37] that the best agreement between the model and the experimental data is if ^{147}Tm is assumed to be triaxial with asymmetry parameter $\gamma \approx 30°$. In the comprehensive theoretical study, using the MPRM approach, of Ref. [38] it was concluded that the level spacings in both the favored and unfavored $\pi h_{11/2}$ bands are best reproduced if ^{147}Tm is triaxially deformed with $\beta_2 = 0.21$ and $\gamma = 25°$. This interpretation is supported by the proton-emission rate of the ground state of ^{147}Tm. For the proton-emitting isomeric state of ^{147}Tm a spin and parity of $5/2^+$ was proposed [38], and it was suggested that the wave function of the $5/2^+$ state is dominated by the $\pi d_{5/2}$ orbital.

The presently obtained precise half-life value of 375(5) μs allows us to confirm the $5/2^+$ assignment, and probe the shape of the isomeric state. In order to facilitate this interpretation, the calculations of Ref. [38] were extended to other possible deformations considering the presently measured proton-decay energy. The calculated partial proton-emission half-lives are compared to the measured one in Fig. 5(a), and they show very good agreement for $0.2 \lesssim \beta_2 \lesssim 0.3$ and $\gamma \lesssim 20°$. However, within the model there is also a $3/2^+$ state close to the Fermi surface. From the calculated internal transition rates the $3/2^+$ state must be above the $5/2^+$ state, otherwise the internal electromagnetic transition would dominate over the proton decay. The energy difference between the states is shown in Fig. 5(b). Consequently, the positive values of the energy difference, shown in red and orange, can be ruled out. This narrows down the possible deformations and practically excludes the pure prolate shape. Within the model the $3/2^+$ state is also proton decaying, but the calculated level structure above it does not match the measured level scheme at any deformation, hence the $3/2^+$ interpretation for the isomeric state can be excluded.

Further support for the triaxial interpretation can be obtained by studying the states feeding the $5/2^+$ isomer. As
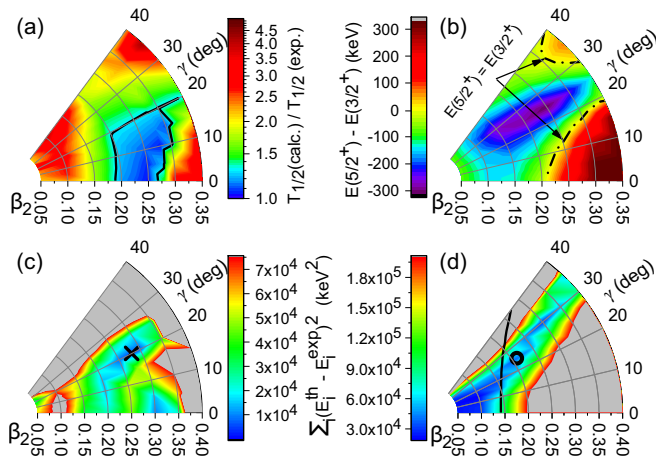
FIG. 5. Results of the nonadiabatic quasiparticle calculations in ^{147}Tm as a function of the deformation: (a) Ratio of the theoretical and measured partial proton-emission half-lives of the $5/2^+$ state. The combined uncertainties of the model total to 30% that is indicated with a black contour. (b) Calculated energy of the $5/2^+$ state with respect to that of the $3/2^+$ state. (c) Sum of squared energy residuals of selected states feeding the $5/2^+$ isomer; the symbol marks the global minimum. (d) Same as (c) but for the states above the $11/2^-$ ground state. Smallest deformations are excluded by the half-life analysis as indicated with the solid line. The open symbol marks the triaxial deformation suggested in Ref. [38].

demonstrated in Figs. 3(a)–3(d), the four most intense γ-ray transitions visible in Fig. 2(b) are mutually anticoincident. This suggests a fragmented band structure above the isomer. The angular distribution coefficients of the 220- and 511-keV transitions point to a dipole character with plausible quadrupole admixture. Therefore, we place $7/2^+$ states in the level scheme at the energies of 288 and 579 keV. All the other transitions are of stretched quadrupole character, and are placed in the level scheme accordingly. In order to interpret the four observed bands a comparison to the MPRM calculations was performed. In this theoretical approach the experimental spectrum of the even-even core is coupled to the quasiparticle states of the odd proton, thus guaranteeing the correct treatment of the Pauli principle. Within the model, levels built on dominant $\pi d_{5/2}$, $\pi s_{1/2}$, and $\pi g_{7/2}$ orbitals are found; see the Supplemental Material [46] for the energies and wave functions of the states. We interpret bands 1 and 2 above the isomer as the favored and unfavored partner of the $\pi d_{5/2}$ band. Similarly, bands 3 and 4 are build on mixed $\pi s_{1/2}$ and $\pi g_{7/2}$ orbitals. In the (β_2, γ) plane there are two regions where we find reasonable agreement[1] between the calculated

---

[1]Here "reasonable agreement" signifies a correct sequence and an energy deviation no more than some hundreds of keV for the calculated states with respect to the measured ones. For many low-lying states the energy residuals are an order of magnitude better, which indicates an excellent agreement. The larger deviation for the high-spin states is due to the unavailability of the experimental energies of the excited states of the even-even core, which are used as an input in the MPRM calculations.
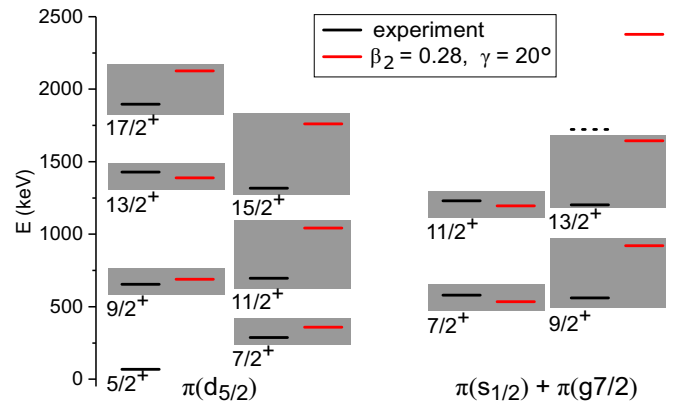

FIG. 6. Comparison of the measured level energies above the proton-decaying $5/2^+$ state to those calculated using the nonadiabatic quasiparticle model. The gray boxes are to group similar states.

and measured level energies of the lowest excited states above the isomer. To visualize this, we show in Fig. 5(c) the sum of squared energy residuals of the $I^\pi \leqslant 13/2^+$ members of the bands 1 and 3 as the model best reproduced the favored bands. Two pronounced minima are found: a local one in the already excluded prolate region and a global, triaxial minimum at $\beta_2 \approx 0.28$ and $\gamma \approx 20°$ which is marked with a symbol in Fig. 5(c). It should be noted that at this triaxial deformation the proton-emission rate of the isomer is reproduced within uncertainties, and the rivaling $5/2^+$ and $3/2^+$ states are in the appropriate order. Following this triaxial ansatz the experimentally and theoretically observed states are grouped and compared in Fig. 6.

For completeness, an identical set of MPRM calculations was performed for the negative parity states of ^{147}Tm, results of which are now briefly summarized. First, the smallest values of β_2 can be excluded by inspecting (not shown here) the partial proton-emission half-life of the ground state; this limit is marked with a black line in Fig. 5(d). Second, the sum of squared energy residuals of the $I^\pi \leqslant 27/2^-$ states feeding the ground state shows a narrow β_2-soft minimum; see Fig. 5(d). This minimum includes the triaxial shape of $\beta_2 = 0.21$ and $\gamma = 25°$ proposed in Ref. [38], as indicated with the open symbol in Fig. 5(d).

In summary, a recoil-decay tagging study of the proton emitting nucleus ^{147}Tm was performed. The present results are in good agreement with the earlier studies [37,38], which showed that the $11/2^-$ ($\pi h_{11/2}$) ground state of ^{147}Tm is likely to be triaxial with $\beta_2 = 0.21$ and $\gamma = 25°$. In the present work the level scheme was expanded above the proton-emitting isomeric $5/2^+$ ($\pi d_{5/2}$) state. The measured proton-decay rate and the level spacings above the isomer were compared to those obtained via nonadiabatic quasiparticle calculations. The isomeric state was found likely to be triaxial with $\beta_2 = 0.28$ and $\gamma = 20°$, seemingly more deformed than the ground state. This is the first instance where proton decay has been used as a tool to probe a shape coexistence candidate. Additionally, evidence was found for a possible shape coexistence of two triaxial shapes. Similarly to ^{151}Lu [19,20], it would be interesting to perform a lifetime measurement for the low-lying levels of ^{147}Tm with a plunger device and a recoil separator.

This would give access to the underlying transition matrix elements, which would provide an additional observable to compare with the theory and discuss the deformation and shape coexistence even further. This type of experiment would be feasible with the techniques available to date.

The experimental data obtained in the present work, and the corresponding metadata, are available [47]. The theoretical results may be acquired directly from P.S., L.S.F., or E.M.

[1] E. M. Burbidge, G. R. Burbidge, W. A. Fowler, and F. Hoyle, Rev. Mod. Phys. **29**, 547 (1957).

[2] M. Arnould, S. Goriely, and K. Takahashi, Phys. Rep. **450**, 97 (2007).

[3] H. Schatz, A. Aprahamian, V. Barnard, L. Bildsten, A. Cumming, M. Ouellette, T. Rauscher, F.-K. Thielemann, and M. Wiescher, Phys. Rev. Lett. **86**, 3471 (2001).

[4] V. V. Elomaa, G. K. Vorobjev, A. Kankainen, L. Batist, S. Eliseev, T. Eronen, J. Hakala, A. Jokinen, I. D. Moore, Y. N. Novikov, H. Penttilä, A. Popov, S. Rahaman, J. Rissanen, A. Saastamoinen, H. Schatz, D. M. Seliverstov, C. Weber, and J. Äystö, Phys. Rev. Lett. **102**, 252501 (2009).

[5] K. Auranen, D. Seweryniak, M. Albers, A. Ayangeakaa, S. Bottoni, M. Carpenter, C. Chiara, P. Copp, H. David, D. Doherty, J. Harker, C. Hoffman, R. Janssens, T. Khoo, S. Kuvin, T. Lauritsen, G. Lotay, A. Rogers, C. Scholey, J. Sethi *et al.*, Phys. Lett. B **792**, 187 (2019).

[6] P. J. Woods and C. N. Davids, Annu. Rev. Nucl. Part. Sci. **47**, 541 (1997).

[7] A. Sonzogni, Nucl. Data Sheets **95**, 1 (2002).

[8] B. Blank and M. Borge, Prog. Part. Nucl. Phys. **60**, 403 (2008).

[9] R. D. Page, EPJ Web Conf. **123**, 01007 (2016).

[10] C. Qi, R. Liotta, and R. Wyss, Prog. Part. Nucl. Phys. **105**, 214 (2019).

[11] B. Blank and R. D. Page, in *Handbook of Nuclear Physics*, edited by I. Tanihata, H. Toki, and T. Kajino (Springer Nature, Singapore, 2020), pp. 1–44.

[12] S. Hofmann, W. Reisdorf, G. Münzenberg, F. P. Heßberger, J. R. H. Schneider, and P. Armbruster, Z. Phys. A **305**, 111 (1982).

[13] O. Klepper, T. Batsch, S. Hofmann, R. Kirchner, W. Kurcewicz, W. Reisdorf, E. Roeckl, D. Schardt, and G. Nyman, Z. Phys. A **305**, 125 (1982).

[14] N. Nica and B. Singh, Nucl. Data Sheets **181**, 1 (2022).

[15] D. T. Doherty, A. N. Andreyev, D. Seweryniak, P. J. Woods, M. P. Carpenter, K. Auranen, A. D. Ayangeakaa, B. B. Back, S. Bottoni, L. Canete, J. G. Cubiss, J. Harker, T. Haylett, T. Huang, R. V. F. Janssens, D. G. Jenkins, F. G. Kondev, T. Lauritsen, C. Lederer-Woods, J. Li *et al.*, Phys. Rev. Lett. **127**, 202501 (2021).

[16] K. Auranen, A. D. Briscoe, L. S. Ferreira, T. Grahn, P. T. Greenlees, A. Herzáň, A. Illana, D. T. Joss, H. Joukainen, R. Julin, H. Jutila, M. Leino, J. Louko, M. Luoma, E. Maglione, J. Ojala, R. D. Page, J. Pakarinen, P. Rahkila, J. Romero *et al.*, Phys. Rev. Lett. **128**, 112501 (2022).

[17] D. Seweryniak, P. J. Woods, J. J. Ressler, C. N. Davids, A. Heinz, A. A. Sonzogni, J. Uusitalo, W. B. Walters, J. A. Caggiano, M. P. Carpenter, J. A. Cizewski, T. Davinson, K. Y. Ding, N. Fotiades, U. Garg, R. V. F. Janssens, T. L. Khoo, F. G. Kondev, T. Lauritsen, C. J. Lister *et al.*, Phys. Rev. Lett. **86**, 1458 (2001).

[18] D. Seweryniak, B. Blank, M. P. Carpenter, C. N. Davids, T. Davinson, S. J. Freeman, N. Hammond, N. Hoteling, R. V. F. Janssens, T. L. Khoo, Z. Liu, G. Mukherjee, A. Robinson, C. Scholey, S. Sinha, J. Shergur, K. Starosta, W. B. Walters, A. Woehr, and P. J. Woods, Phys. Rev. Lett. **99**, 082502 (2007).

[19] M. Procter, D. Cullen, M. Taylor, G. Alharshan, L. Ferreira, E. Maglione, K. Auranen, T. Grahn, P. Greenlees, U. Jakobsson, R. Julin, A. Herzáň, J. Konki, J. Leino, J. Pakarinen, J. Partanen, P. Peura, P. Rahkila, P. Ruotsalainen, M. Sandzelius *et al.*, Phys. Lett. B **725**, 79 (2013).

[20] M. J. Taylor, D. M. Cullen, M. G. Procter, A. J. Smith, A. McFarlane, V. Twist, G. A. Alharshan, L. S. Ferreira, E. Maglione, K. Auranen, T. Grahn, P. T. Greenlees, K. Hauschild, A. Herzan, U. Jakobsson, R. Julin, S. Juutinen, S. Ketelhut, J. Konki, M. Leino *et al.*, Phys. Rev. C **91**, 044322 (2015).

[21] P. Siwach, P. Arumugam, S. Modi, L. S. Ferreira, and E. Maglione, Phys. Rev. C **106**, 044322 (2022).

[22] P. Arumugam, L. Ferreira, and E. Maglione, Phys. Lett. B **680**, 443 (2009).

[23] P. Siwach, P. Arumugam, S. Modi, L. S. Ferreira, and E. Maglione, Phys. Rev. C **105**, L031302 (2022).

[24] P. Arumugam, L. S. Ferreira, and E. Maglione, Phys. Rev. C **78**, 041305(R) (2008).

[25] P. J. Woods, P. Munro, D. Seweryniak, C. N. Davids, T. Davinson, A. Heinz, H. Mahmud, F. Sarazin, J. Shergur, W. B. Walters, and A. Woehr, Phys. Rev. C **69**, 051302(R) (2004).

[26] P. Möller, A. Sierk, R. Bengtsson, H. Sagawa, and T. Ichikawa, At. Data Nucl. Data Tables **98**, 149 (2012).

[27] S. Hilaire and M. Girod, Eur. Phys. J. A **33**, 237 (2007).

[28] S. Hilaire and M. Girod, AMEDEE database, accessed 03.11.2022, https://www-phynu.cea.fr/science_en_ligne/carte_potentiels_microscopiques/carte_potentiel_nucleaire_eng.htm.

[29] K. Heyde, P. Van Isacker, M. Waroquier, J. Wood, and R. Meyer, Phys. Rep. **102**, 291 (1983).

[30] J. Wood, K. Heyde, W. Nazarewicz, M. Huyse, and P. van Duppen, Phys. Rep. **215**, 101 (1992).

[31] K. Heyde and J. L. Wood, Rev. Mod. Phys. **83**, 1467 (2011).

[32] R. Julin, T. Grahn, J. Pakarinen, and P. Rahkila, J. Phys. G: Nucl. Part. Phys. **43**, 024004 (2016).

[33] P. E. Garrett, M. Zielińska, and E. Clément, Prog. Part. Nucl. Phys. **124**, 103931 (2022).

[34] A. N. Andreyev, M. Huyse, P. V. Duppen, L. Weissman, D. Ackermann, J. Gerl, F. P. Heßberger, S. Hofmann, A. Kleinböhl, G. Münzenberg, S. Reshitko, C. Schlegel, H. Schaffner, P. Cagarda, M. Matos, S. Saro, A. Keenan, C. Moore, C. D. O'Leary, R. D. Page *et al.*, Nature (London) **405**, 430 (2000).

[35] J. Ojala, J. Pakarinen, P. Papadakis, J. Sorri, M. Sandzelius, D. M. Cox, K. Auranen, H. Badran, P. J. Davies, T. Grahn, P. T. Greenlees, J. Henderson, A. Herzáň, R.-D. Herzberg, J. Hilton, U. Jakobsson, D. G. Jenkins, D. T. Joss, R. Julin, S. Juutinen *et al.*, Commun. Phys. **5**, 213 (2022).

[36] D. Seweryniak, C. N. Davids, W. B. Walters, P. J. Woods, I. Ahmad, H. Amro, D. J. Blumenthal, L. T. Brown, M. P. Carpenter, T. Davinson, S. M. Fischer, D. J. Henderson, R. V. F. Janssens, T. L. Khoo, I. Hibbert, R. J. Irvine, C. J. Lister, J. A. Mackenzie, D. Nisius, C. Parry *et al.*, Phys. Rev. C **55**, 2137(R) (1997).

[37] D. Seweryniak, C. N. Davids, A. Robinson, P. J. Woods, B. Blank, M. P. Carpenter, T. Davinson, S. J. Freeman, N. Hammond, N. Hoteling, R. V. F. Janssens, T. L. Khoo, Z. Liu, G. Mukherjee, J. Shergur, S. Sinha, A. A. Sonzogni, W. B. Walters, and A. Woehr, Eur. Phys. J. A **25**, 159 (2005).

[38] S. Modi, M. Patial, P. Arumugam, L. S. Ferreira, and E. Maglione, Phys. Rev. C **96**, 064308 (2017).

[39] J. Pakarinen, J. Ojala, P. Ruotsalainen, H. Tann, H. Badran, T. Calverley, J. Hilton, T. Grahn, P. T. Greenlees, M. Hytönen, A. Illana, A. Kauppinen, M. Luoma, P. Papadakis, J. Partanen, K. Porras, M. Puskala, P. Rahkila, K. Ranttila, J. Sarén *et al.*, Eur. Phys. J. A **56**, 149 (2020).

[40] J. Sarén, J. Uusitalo, M. Leino, P. T. Greenlees, U. Jakobsson, P. Jones, R. Julin, S. Juutinen, S. Ketelhut, M. Nyman, P. Peura, P. Rahkila, C. Scholey, and J. Sorri, Nucl. Instrum. Methods Phys. Res. Sect. B **266**, 4196 (2008).

[41] J. Uusitalo, J. Sarén, J. Partanen, and J. Hilton, Acta Phys. Pol. B **50**, 319 (2019).

[42] P. Rahkila, Nucl. Instrum. Methods Phys. Res., Sect. A **595**, 637 (2008).

[43] K. H. Schmidt, Eur. Phys. J. A **8**, 141 (2000).

[44] R. Simon, K. Schmidt, F. Heßberger, S. Hlavac, M. Honusek, G. Münzenberg, H.-G. Clerc, U. Gollerthan, and W. Schwab, Z. Phys. A **325**, 197 (1986).

[45] E. S. Paul, P. J. Woods, T. Davinson, R. D. Page, P. J. Sellin, C. W. Beausang, R. M. Clark, R. A. Cunningham, S. A. Forbes, D. B. Fossan, A. Gizon, J. Gizon, K. Hauschild, I. M. Hibbert, A. N. James, D. R. LaFosse, I. Lazarus, H. Schnare, J. Simpson, R. Wadsworth *et al.*, Phys. Rev. C **51**, 78 (1995).

[46] See Supplemental Material at http://link.aps.org/supplemental/10.1103/PhysRevC.108.L011303 for the measured γ-ray data and the results of the nonadiabatic quasiparticle calculations.

[47] Data are available at https://doi.org/10.23729/65298853-0ec8-4728-a981-8b44bad7c467.